

Article

Test and Optimization of Oilseed Rape (*Brassica napus* L.) Threshing Device Based on DEM

Jun Wu, Qing Tang, Senlin Mu, Lan Jiang and Zhichao Hu *

Nanjing Institute of Agricultural Mechanization, Ministry of Agriculture and Rural Affairs, Nanjing 210014, China

* Correspondence: huzhichao@caas.cn

Abstract: Gridded concave plate sieves are usually used for threshing operations of grain and oilseed crops. In response to the problems of high threshing loss rate and grain breakage rate when threshing oilseed rape, this research modified the threshing concave plate of oilseed rape (*Brassica napus* L.) harvesters to improve the performance and efficiency of oilseed rape separation. The improved threshing concave plate adopts a 360° wrap angle, and a guide plate with an adjustable inflow angle is designed on the inner side of the concave plate. The optimal combination of parameters for the threshing device is determined by simulation analysis and field testing. Single-factor simulations of the threshing cylinder speed and guide plate angle are carried out using EDEM, which showed that both are influencing factors for the force and speed of the oilseed rape particles. A three-factor and three-level orthogonal experiment was undertaken to validate the simulation analysis further. The threshing cylinder speed, concave plate speed, and guide plate angle were influencing factors. The threshing loss rate and grain breakage rate are evaluation indicators. The field validation tests are carried out on concave plates with 180° wrap angle and 360° wrap angle, the results showed that the concave plate with 360° wrap angle reduces the threshing loss rate by 4.25%, the grain breakage rate by 0.93%, and improved the harvesting efficiency by 0.31 km/h when the threshing cylinder speed was 81.89 rad/s, concave plate speed was 9.34 rad/s, and guide plate angle was 40°. This study demonstrates that the concave plate with a 360° wrap angle has better performance and operational efficiency, and it provides design ideas for threshing devices for other crop combine harvesters.

Keywords: oilseed rape (*Brassica napus* L.); threshing concave plate; discrete element method; design; experiment



Citation: Wu, J.; Tang, Q.; Mu, S.; Jiang, L.; Hu, Z. Test and Optimization of Oilseed Rape (*Brassica napus* L.) Threshing Device Based on DEM. *Agriculture* **2022**, *12*, 1580. <https://doi.org/10.3390/agriculture12101580>

Academic Editor: Yanbo Huang

Received: 8 August 2022

Accepted: 21 September 2022

Published: 30 September 2022

Publisher's Note: MDPI stays neutral with regard to jurisdictional claims in published maps and institutional affiliations.



Copyright: © 2022 by the authors. Licensee MDPI, Basel, Switzerland. This article is an open access article distributed under the terms and conditions of the Creative Commons Attribution (CC BY) license (<https://creativecommons.org/licenses/by/4.0/>).

1. Introduction

Oilseed rape (*Brassica napus* L.) is one of the major oil crops, and China is a major oilseed rape producer with a planted area of 6765 thousand hectares and a production of 14,049 million tons in 2021 [1]. Oilseed rape harvesting has been dominated by manual harvesting, with a low degree of mechanization. Restricted by harvesting methods and planting patterns, people's increasing consumption levels and expanding production require new requirements and efficiency for efficient and low-loss oilseed rape harvesting. The loss caused by rape harvest is mainly the interference of harvesting machinery on crops, and the backwardness of harvesting means has become the main factor limiting the large-scale cultivation of rape. Whether the complete rapeseed grains can be harvested in the appropriate harvest period directly affects the quality of rape [2,3]. The harvesting environment of oilseed rape threshing is very complicated, and the current threshing device leads to a high threshing loss rate, high grain breakage rate, and low production efficiency. Previous studies have shown that harvest breakage occurs mainly in the threshing process. The impact of threshing components can cause the seeds to break. Hobson et al. [4] proposed that the cracking angle of rape siliques at the mature stage would lead to the total grain loss accounting for a quarter of the total yield. Changing the structure and operating

parameters of the threshing device can effectively reduce grain breakage. So, it is essential to study the damage of oilseed rapeseed threshing for its utilization.

The HeGe 160 and 180 series oilseed rape harvesters produced by the German company Hege and the tracked self-propelled full-feed axial threshing combine produced by the Japanese company Yanmar are not effective for testing in the hilly and mountainous areas of China due to the limitations of the terrain and the region, they cannot meet the needs of users [5]. Therefore, researchers have conducted some studies on threshing and separation mechanisms and equipment in oilseed rape and other crop harvesting operations and have made breakthroughs.

At present, the most common form of threshing concave is the grid threshing concave [6]. The wrap angle of this concave plate is only 180° , which is installed under the threshing cylinder, and the threshed grains will fall from the grid. However, this concave is easily blocked under the condition of a large feed rate, which will affect the operational performance of the combine harvester. Therefore, there are some studies on adjusting the gap between concave plates [7,8]. In addition, some scholars have developed a device with an automatic adjustment function. Regier et al. [9] and Bergkamp et al. [10] designed a motorized concave sieve with an adjustable concave, which controls the telescoping of the electric actuator on the concave sieve by the feedback value of the displacement sensor, thus changing the up-and-down motion of the concave plate. Morgan et al. [11] put forward a method of testing and evaluating the crack resistance of rape pods by the random collision of steel balls. Still, the testing equipment of this method has a simple structure but low precision. Most of the existing oilseed rape threshing devices on the market refer to mature threshing devices for wheat, rice, and corn. However, due to the significant difference in biomechanical characteristics between oilseed rape and rice and wheat, many grains are lost and broken in actual operation.

Previous studies have mainly focused on concave clearance adjustment and the threshing drum speed control method. As the essential structure with the most significant direct contact area with crops, there are few reports on the innovative design of the structure. There is also a lack of basic research on the contact characteristics between oilseed rape plants and threshing concave. In the design of threshing devices for other crops, more and more scholars apply discrete element method (DEM) technology to carry out their work. The DEM was first put forward by Dr. Cundall [12]. DEM regards the physical material with continuous medium characteristics as many systems composed of discrete elements. Calculating the position and velocity of each unit reflects many microscopic physical laws that are difficult to observe by ordinary experimental means. In recent years, DEM simulation technology has been used more and more in biology, materials, agriculture, and mining. It has become a hot research focus to explore the energy transfer, interaction, and product design among substances by using DEM.

In a discrete system, the force and motion criterion between particles follow the second Newton's law [13]. The adhesion, gravity, and friction of each particle are calculated to obtain the particle's linear velocity and angular velocity, and the position and state of the particle are updated with a fixed time step. For the modeling of agricultural materials, Lenaerts et al. [14] established a segmented flexible straw model, in which linear springs-dampers connected particle units to simulate straw bending stiffness and energy dissipation under shock. Liu et al. [15] established the flexible discrete element model of wheat hollow short straws based on the discrete element method and conducted a series of parameter calibration experiments. Most of these flexible models are built by Hertz–Mindlin with a bonding contact model. In discrete element simulation, the accuracy of the model directly impacts the simulation results. Still, too complicated models will increase the computational complexity and make the simulation results counterproductive, so it is necessary to simplify the model appropriately.

Most of the existing threshing devices use concave plates with 180° wrap angle, in which it is easy to block the cylinder, the threshing is not clean, and the separation is incomplete [16–18]. The threshing breakage of oilseed rape is easily affected by other plant

attributes, such as pod angle, length, and width [19,20], so it is necessary to establish a simulation model with natural rape plants. In this study, a rotatable threshing concave plate with a 360° wrap angle was designed innovatively. The discrete element simulation model of oilseed rape plants was also established by using DEM, carried out single factor experiments of key parameters to explore the movement characteristics of oilseed rape plants during threshing, and carried out single factor experiments of key parameters to assist in determining the key parameters of threshing concave. In addition, the central composite design (CCD) experiment was used to carry out the multi-objective optimization field experiment, the regression model between the evaluation indexes and the influencing factors was established, to analyze the influence law on indexes and obtain the optimal combination of operating parameters.

2. Materials and Methods

2.1. Oilseed Rape Plant Model Based on DEM

DEM is a general method for analyzing the motion process of granular materials [21,22]. The primary purpose of modeling oilseed rape plants is to analyze the kinematic parameters such as power consumption, velocity, and force acting on the particles during the threshing process. To improve the simulation efficiency and reduce the model error, the discrete element model of the oilseed rape plant is simplified to the composition of stalk and ear, and the influence of oilseed rape pods on the threshing process is ignored [16,23].

In this study, Ningza 1818 was selected as the research object, and 100 oilseed rape plants were randomly selected. The average plant height, stubble height, first branch height, straw outer diameter, and inner diameter were 1400 mm, 195 mm, 602 mm, 7.03 mm, and 6.12 mm, respectively. The branch length was 61.3 mm, the outer diameter was 3.5 mm, and the inner diameter was 2.87 mm. In discrete element simulation software, although the closer the model is to the actual object, the more accurate the simulation results will be, this will cause a huge amount of calculation and even lead to the collapse of the calculation software. Therefore, it is necessary to establish a simplified model to avoid this problem. In the research of Ghodki et al. [24], the model of black pepper seed was established as an independent individual bonded by many spherical particles through Hertz–Mindlin with bonding, they omitted the structure of seed coat and endosperm. Wang et al. [25] simplified the straw of citrus fruits into a cylindrical model. Su et al. [7] also proposed a simplified method for the discrete element model of rice, these studies show that the simplified model can also well reflect the characteristics of actual materials, which provides a reference for establishing the rape plant model. The oilseed rape stalk is simplified as a hollow cylinder with a uniform wall area and length, as shown in Figure 1. Here, 4950 spherical particles connect the stalk model with Hertz–Mindlin with the bonding contact model as the bonding bond, and the bonding bond of the stalk model reflects the flexible characteristics of the actual stalk. The oilseed rape ears are distributed on the stalk's left and right sides and consist of branches and seeds. The branches are constructed the same way as the stalk model, while the seed model is built by particle splicing, consisting of one sphere with a radius of 1.5 mm and two spheres with a radius of 1.0 mm.

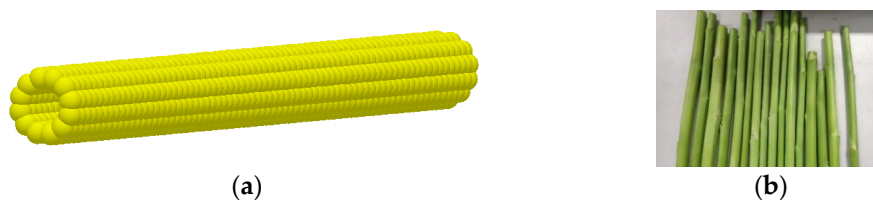


Figure 1. Oilseed rape stalk. (a) Model of oilseed rape stalk. (b) Actual oilseed rape stalk.

The particle–particle bonding force follows the Hertz contact theory. To simulate the contact characteristics when the oilseed rape plant interacted more accurately with the machine, the normal and tangential features of two adjacent spherical particles are shown

in Equations (1)–(4). The Hertz–Mindlin with bonding contact model is used for both particles and particles, and the bonding parameters are shown in Table 2 [26,27].

$$\delta F_n = -v_n S_n \pi R^2 \delta_t \tag{1}$$

$$\delta F_t = -v_t S_t \pi R^2 \delta_t \tag{2}$$

$$\delta M_n = -\frac{1}{2} \omega_n S_t \pi R^4 \delta_t \tag{3}$$

$$\delta M_t = -\frac{1}{4} \omega_n S_t \pi R^4 \delta_t \tag{4}$$

where R is the radius of bonding bond, mm; $F_{n,t}$ is normal and tangential force of particles, N; $S_{n,t}$ is normal and tangential stiffnesses; δ_t is timestep, s; $\omega_{n,t}$ is normal and tangential angular velocities, rad/s; $M_{n,t}$ is normal and tangential moment of particles, N·m.

When the parameters of the bonding bonds between the particles reach the critical value, all the links between the particles disappear so that the particles will recover the discrete characteristics. The critical importance of the bonding bonds is shown in Equations (5) and (6) [28,29]. The characteristic parameters of the particle stalks and bond bonds are shown in Tables 1 and 2, and the simulation model of the oilseed rape plant is shown in Figure 2.

$$\sigma_{\max} \leq -\frac{F_n}{\pi R^2} + \frac{M_t}{\pi R^4} R \tag{5}$$

$$\tau_{\max} \leq -\frac{F_t}{\pi R^2} + \frac{2M_n}{\pi R^4} R \tag{6}$$

Table 1. Parameters of bonding bonds.

Parameters	Value
Normal stiffness per unit area (N·m ⁻²)	8 × 10 ⁸
Shear stiffness per unit area (N·m ⁻²)	6 × 10 ⁸
Critical normal stress (Pa)	1 × 10 ⁸
Critical shear stress (Pa)	9 × 10 ⁷

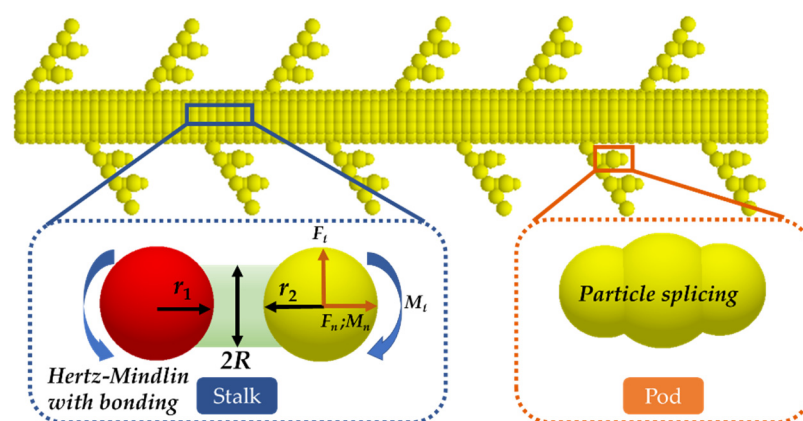


Figure 2. Illustration of the oilseed rape bond.

To obtain a simulation model of oilseed rape plants, 100 oilseed rape plants were selected, and the plant length, ear length, and stalk diameter were measured. The biometric parameters of oilseed rape plants are shown in Table 3.

Table 2. Mechanical properties of the oilseed rape [30–33].

Part of Oilseed Rape	Parameters	Value
Stalk	Passion's ratio	0.4
	Shear modulus (Pa)	7.5×10^5
	Density ($\text{kg}\cdot\text{m}^{-3}$)	240
Primary branch	Passion's ratio	0.4
	Shear modulus (Pa)	7.5×10^5
	Density ($\text{kg}\cdot\text{m}^{-3}$)	240
Pod	Passion's ratio	0.25
	Shear modulus (Pa)	1×10^8
	Density ($\text{kg}\cdot\text{m}^{-3}$)	2500
Stalk-stalk	Coefficient of restitution	0.28
	Coefficient of static friction	0.38
	Coefficient of rolling friction	0.01
Stalk-branch	Coefficient of restitution	0.28
	Coefficient of static friction	0.38
	Coefficient of rolling friction	0.01
Stalk-pod	Coefficient of restitution	0.5
	Coefficient of static friction	0.5
	Coefficient of rolling friction	0.01
Branch-branch	Coefficient of restitution	0.3
	Coefficient of static friction	0.4
	Coefficient of rolling friction	0.01
Branch-pod	Coefficient of restitution	0.5
	Coefficient of static friction	0.5
	Coefficient of rolling friction	0.01
Pod-pod	Coefficient of restitution	0.5
	Coefficient of static friction	0.5
	Coefficient of rolling friction	0.01

Table 3. Characteristics parameters of oilseed rape plant.

Part of Oilseed Rape	Parameters	Value
Stalk	Length of stalk (mm)	600
	Radius (mm)	35
	Diameter of particles (mm)	0.8
Primary branch	Length of primary branch (mm)	60
	Radius (mm)	20
	Diameter of particles (mm)	0.5
Pod	Length of pod (mm)	10
	Number of pods	3
	Maximum diameter of pod	1.5
	Minimum diameter of pod	1.0

2.2. Modeling of the Threshing Device

The oilseed rape threshing device includes the threshing concave plate and threshing cylinder, as shown in Figure 3. The threshing concave plate is a grid-type concave plate, and the guide plate angle is designed to be 360° , effectively improving the threshing efficiency. The threshing concave plate consists of four groups of concave plate sieves connected by a circular support ring. Each set of concave plate sieves consists of three sieves held together by rectangular connecting plates. This design makes the installation and removal of the threshing concave plate easier and facilitates maintenance.

Considering the size of the feeding volume, size of oilseed rape seeds, and other parameters, the length of the sieve holes of the concave plate is 35 mm and the width is 15 mm, and each concave plate sieve is distributed with 360 holes. In addition, the first two groups of concave plate sieves are installed with angle-adjustable deflector plates, as shown in Figure 4.

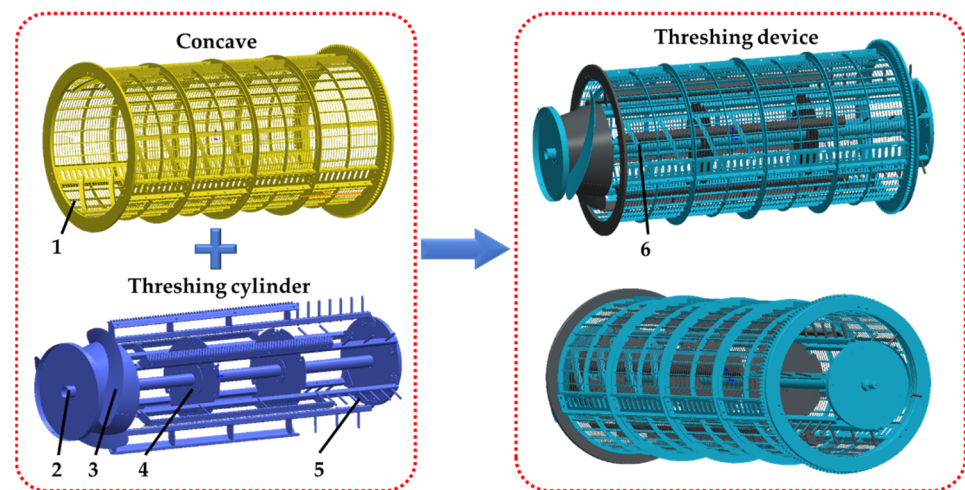


Figure 3. Structure of oilseed rape threshing device. 1—concave; 2—shaft; 3—screw feeding head; 4—spreading disc; 5—threshing elements; 6—guide plate angle.

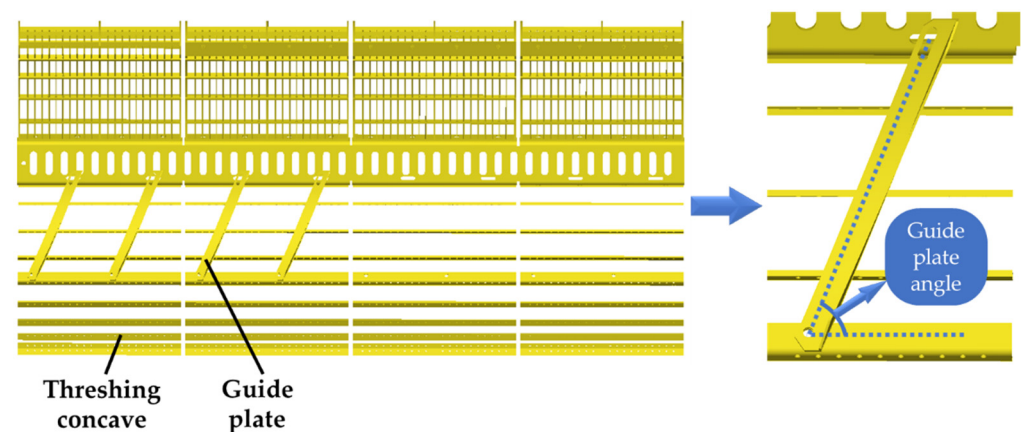


Figure 4. Structure of threshing concave plate.

Suppose the guide plate angle is too small. In that case, the materials stay in the threshing device for too long, and the impurities cannot be discharged out of the machine in time, which will quickly lead to the problem of clogging the threshing cylinder and a high breakage grain rate. Suppose the angle of the guide plate angle is too large. In that case, the axial conveying speed of the oilseed rape plant is too large, which will shorten the contact time between the oilseed rape and other threshing elements, resulting in insufficient threshing operation and a high threshing loss rate.

Therefore, the guide plate angle design is one of the main influencing factors in threshing operation. The threshing cylinder consists of a shaft, spreading discs, a screw feeding head, and threshing elements. The shaft is connected to three discs, and the threshing elements are fixed evenly on the circumference of the discs utilizing square steel. The oilseed rape threshing method adopts the compound threshing form of “long ribs + spike teeth,” with six groups of threshing elements, each including one long rib and six spike teeth. The role of the long ribs is to strip the oilseed rape seeds from the angular fruits, and the part of the peg teeth is to discharge the oilseed rape stalks and other impurities outside the device. The length of the long striker is 750 mm, the height is 90 mm, the spacing of the peg teeth is 80 mm, and the size is 90 mm [33].

2.3. Details of the Simulation

The oilseed rape threshing process feeds multiple bunches of oilseed rape plants into the threshing device, as shown in Figure 5. The feeding area is used to feed oilseed rape

plants, the threshing area is used to thresh, and the miscellaneous area is where impurities such as hulls and broken stalks are discharged out of the device. We set the feeding speed to 7.5 km/h, removing the limit constraint effect on the particles when the bonding bond is generated, and adding the global gravitational acceleration to 9.8 N/kg. After the oilseed rape plant is fed into the threshing device, it first enters the threshing zone, where the oilseed rape seeds fall off the spike shaft and become discrete particles under the action of the threshing ribs and concave plates [14]. The threshed seeds fall into the catch box under inertia. The operating environment of the threshing simulation is shown in Table 4.

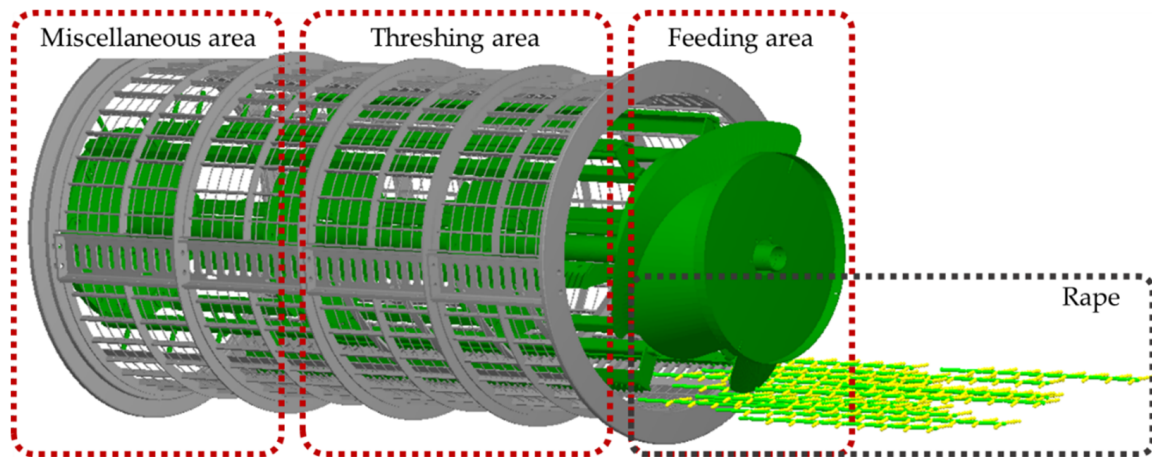


Figure 5. Initialization of oilseed rape threshing simulation.

Table 4. Simulation environment.

Projects	Value
Software version	EDEM 2020
CPU	3.2 GHz Intel i7-8700
RAM	16 G
Calculate step	3.5×10^{-6} (s)
Calculation duration	28 (h)

2.4. Field Test Method

The oilseed rape harvesting field test was conducted in Liyang City, Jiangsu Province, from 6–8 June 2022. The test scheme is shown in Table 5. In this test, the threshing cylinder speed, concave plate speed, and guide plate angle are independent variables, and threshing loss rate and grain breakage rate are evaluation indexes. The oilseed rape harvest field test is carried out according to “GB/T8097-2008 Test Method of Harvesting Machinery Combine Harvester” and “NY/T1231-2006 Technical Specification for Quality Evaluation of Oilseed rape Combine Harvester”, as shown in Figure 6.

Table 5. Scheme of field test.

Parameters	A-Threshing Cylinder Speed ($\text{rad}\cdot\text{s}^{-1}$)	B-Concave Plate Speed ($\text{rad}\cdot\text{s}^{-1}$)	C-Guide Plate Angle ($^{\circ}$)
−1	500	50	30
0	700	100	40
1	900	150	50



Figure 6. Oilseed rape harvest. (a) World oilseed rape combine harvester. (b) Test Sample collection.

Ningza 1818 oilseed rapeseed was planted in the test area. The area was divided into preparation, test, and parking areas. The length of the preparation area and the parking area were 10 m, the length of the test area was 20 m, the harvester only works in the preparation area and test area, stubble height was consistent, and the speed and other conditions in the experiments were not changed during the test. After the test, all the materials in the hopper were discharged to the receiving box outside the machine, and 200 g samples (1 kg in total) were randomly taken out by the five-point sampling, to count the threshing loss rate and grain breakage rate. Design Expert was used to design the test scheme, and 17 groups of tests were carried out in total. Each group of tests was repeated three times, and the average value was taken.

3. Results and Discussion

3.1. Simulation Results

3.1.1. Influence of Guide Plate Angle on the Movement Characteristics of Particles

There are few references about the design of the angle of the guide plate of the threshing device. This study is the first application of DEM to the simulation of the oilseed rape threshing device. The simulation was carried out on the guide plate angle at 30° , 40° , and 50° , the operating conditions were such that only the threshing cylinder rotated at 15.71 rad/s, and the concave plate remained relatively stationary.

Table 6 shows the mean and standard deviation results. Figure 7 shows the simulation results for the oilseed rape seed threshing. When threshing rapeseed, it is required to thresh as much oilseed rape as successfully possible, so as to increase the yield and increase farmers' income [32]. However, some losses will inevitably occur in the threshing process, which is related to the guide plate angle. The smaller the guide plate angle is in actual harvest, the greater the threshing loss may be caused. According to the waveform of the force, the velocity of particles, and seed-stalk bonding bond breaking force, with the increase of the angle of the guide plate, the fluctuation of each numerical value gradually becomes more significant, and the maximum value exceeds 250 N. This change leads to the poor axial fluidity of the particles, and the threshing elements repeatedly impact the particles during threshing. This result provides a reference for determining the angle of the guide plate.

Figure 8a,b shows the force, velocity, and breaking force of the seed-stalk over time for guide plate angles of 30° , 40° , and 50° , respectively. The simulation results show that different deflector angles influence particles' movement. At first, when the guide plate angle is small, the residence time of oilseed rape plants in the threshing device is the shortest, which means that the force of rape particles is the smallest, the movement speed of particles, and the breaking force of bonding bond with particle-straw are also the smallest. Although this reduces the occurrence of crushing, a few particles still cannot entirely fall

off the straw, resulting in threshing loss. With the increase in the guide plate angle, oilseed rape plants cannot be quickly transported to the other side of the threshing drum along the guide plate. They stay in the threshing device and collide and impact with the threshing element and concave plate many times, which makes the force of particles larger and the movement speed also increases, but this is beneficial in terms of threshing more fully and reducing the loss rate.

Table 6. Simulation results in different guide plate angle.

Level	Project	Force of the Particles (N)	Velocity of Particles (km·h ⁻¹)	Seed-Stalk Bonding Bond Breaking Force (N)
30°	Average	155.41	33.3	73.63
	Standard deviation	29.5	13.14	26.64
40°	Average	183.03	52.70	75.69
	Standard deviation	25.15	16.49	34.07
50°	Average	202.04	67.46	73.79
	Standard deviation	43.52	17.71	36.22

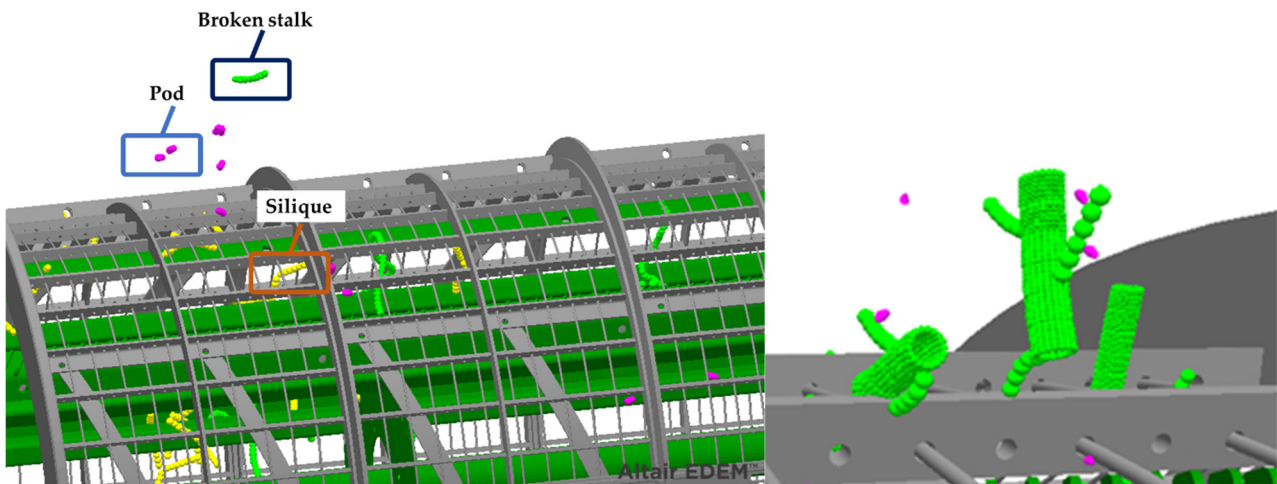


Figure 7. Force cloud diagram of different type of particles.

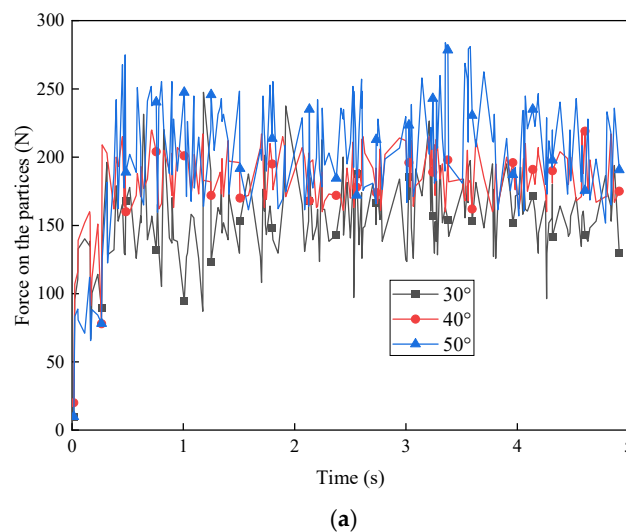


Figure 8. Cont.

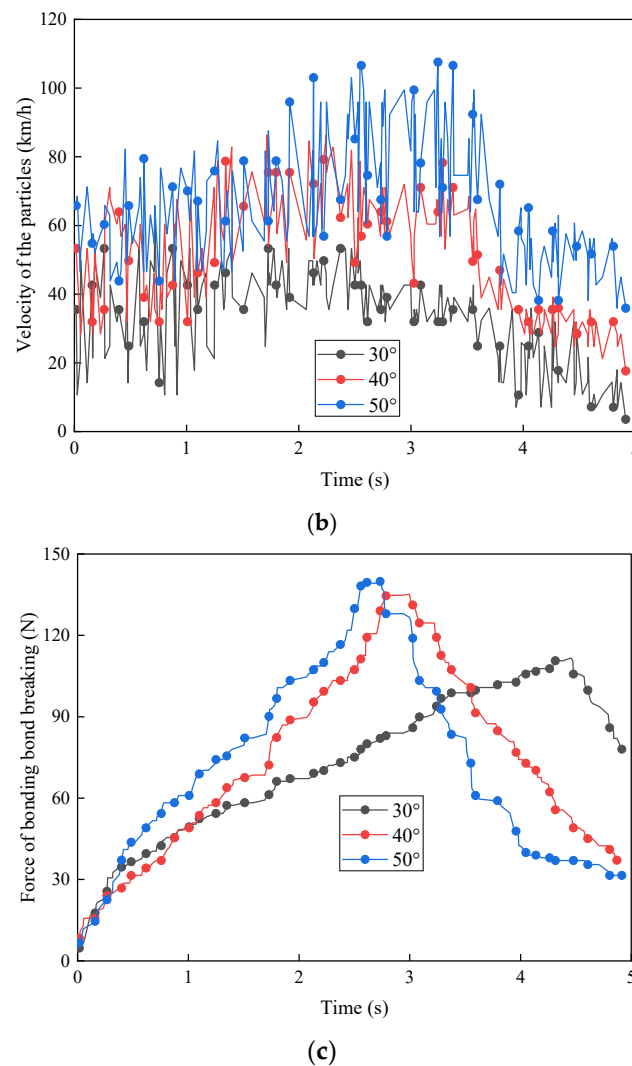


Figure 8. Influence of different guide plate angle on the particles. (a) Force curves of particles. (b) Velocity curves of particles. (c) Breaking force curves of the seed-stalk bonding bond.

3.1.2. Influence of Concave Speed on the Movement Characteristics of Particles

The traditional threshing plate comprises a 180° grating concave plate and a closed upper concave plate. For example, according to the study of Bergkamp et al. [10] and Miu et al. [33], the threshed grains are discharged from the concave grid by gravity. In contrast, the concave plate proposed in this study adopts a 360° guide plate, which increases the contact area between oilseed rape plants and the concave plate by two times and greatly improves the threshing efficiency [34].

The concave speed also has a significant effect on the kinematic state of the particles, as shown in Table 7. In Figure 9, with the stress distribution program of green particles representing oilseed rape stalks and yellow particles representing oilseed rape grains under the combined action of threshing elements and threshing concave plates, the oilseed rape plants enter the threshing device and make a circular spiral motion along the guide plate. The concave plate speed also had a significant effect on the state of motion of the particles, and the simulation results are shown in Figure 10a–c when the concave plate started working at different speeds. This study is also the first to use DEM to analyze the influence of rotating threshing concave on threshing performance. The results show that the rotating threshing concave plate accelerates the threshing process. With the increasing rotating speed of the threshing concave plate, the force on the particles is constantly increasing, but the movement speed of the particles is decreasing, at the same time, the numerical

fluctuation is gradually drastic. It is because the larger concave plate speed increases the collision between particles, but it also eliminates the moving speed of particles given by the threshing cylinder. It is because the threshing concave plate counteracts the linear speed given to the particles by the threshing cylinder, which makes the rape thresh at a lower movement speed, which helps to reduce the crushing rate and loss rate. It indicates that the rotating concave plate can enhance the threshing ability to a certain extent. At present, there is no research conclusion about rotating threshing concave plates for reference and this conclusion needs further verification by field experiments.

Table 7. Simulation results in different concave plate speed.

Level	Project	Force of the Particles (N)	Velocity of Particles ($\text{km}\cdot\text{h}^{-1}$)	Pod-Stalk Bonding Bond Breaking Force (N)
5.24 (rad/s)	Average	89.55	75.67	78.84
	Standard deviation	35.31	34.78	31.24
10.47 (rad/s)	Average	96.87	60.98	85.34
	Standard deviation	30.65	20.41	28.43
15.71 (rad/s)	Average	121.32	39.38	97.65
	Standard deviation	33.18	26.17	36.55

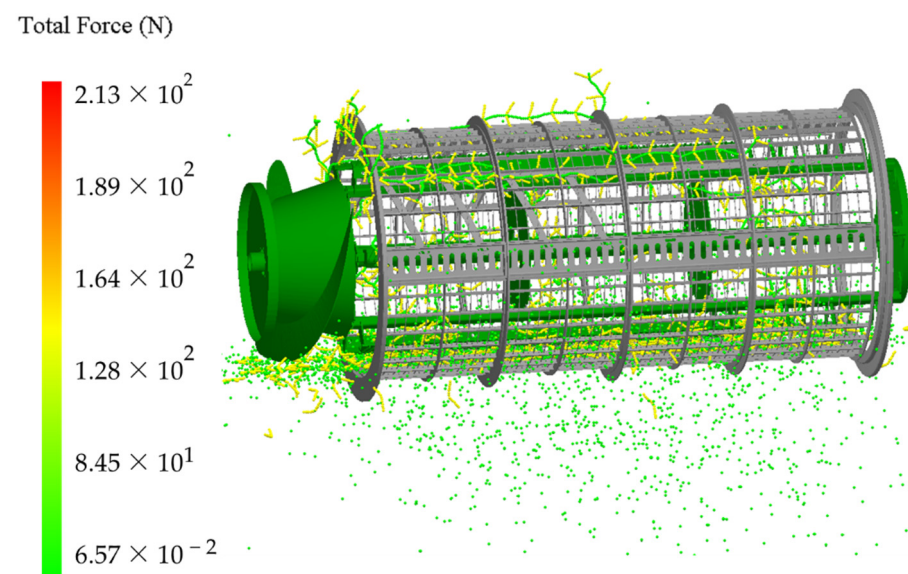


Figure 9. Force cloud diagram of different type of particles.

3.2. Field Test Results and Analysis

As seen in Table 5, a three-way analysis of variance (ANOVA) at significance level 0.05 was used to establish the effect of threshing cylinder speed, concave plate speed, and guide plate angle on threshing loss rate and grain breakage rate [35]. Table 8 shows the oilseed rape threshing test results. Table 9 shows ANOVA results of grain threshing loss rate, and Table 10 shows ANOVA results of grain breakage rate.

In Tables 9 and 10, the p -value reflects the degree of significance of each factor in the model on the evaluation indicators. $p < 0.01$ indicates that this factor has a highly significant influence, $0.01 < p < 0.05$ suggests that this factor has a significant influence and $p > 0.05$ means that this factor has no effect [36,37]. The main indexes to judge whether the regression model is effective include the p -value of the model, the p -value of the Lack of fit terms, the regression coefficient R^2 of the model, and so on.

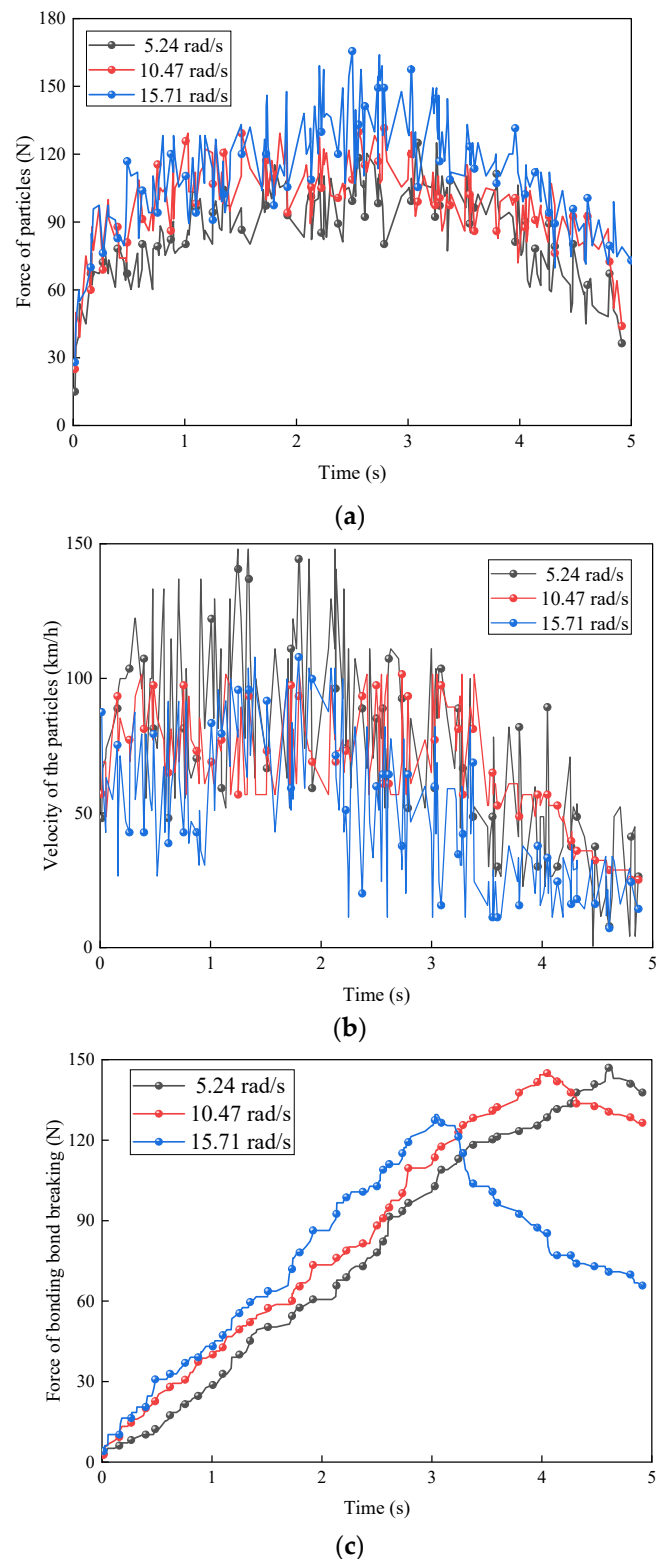


Figure 10. Variation of kinematic characteristics of particles with time in different concave plate speed. (a) Force curves of particles. (b) Velocity curves of particles. (c) Breaking force curves of the seed-stalk bonding bond.

Table 8. The oilseed rape threshing test results.

Test Number	A—Threshing Cylinder Speed	B—Concave Plate Speed	C—Guide Plate Angle	Threshing Loss Rate/%	Grain Breakage Rate/%
1	−1	−1	0	4.272	0.883
2	1	−1	0	3.878	0.913
3	−1	1	0	4.254	0.917
4	1	1	0	3.851	0.922
5	−1	0	−1	4.231	0.902
6	1	0	−1	3.836	0.905
7	−1	0	1	4.315	0.874
8	1	0	1	3.903	0.896
9	0	−1	−1	4.078	0.864
10	0	1	−1	3.995	0.891
11	0	−1	1	4.173	0.842
12	0	1	−1	4.123	0.862
13	0	0	0	4.093	0.859
14	0	0	0	4.111	0.858
15	0	0	0	4.107	0.858
16	0	0	0	4.11	0.867
17	0	0	0	4.088	0.853

Table 9. ANOVA of the oilseed rape threshing loss rate.

Source	Standard Deviation	Freedom	Sum of Squares	F Value	p Value	Significant Degree
Regression model	0.35	9	0.039	130.26	<0.0001	***
A	0.32	1	0.32	1084.77	<0.0001	***
B	3.960×10^{-3}	1	3.960×10^{-3}	13.36	0.0081	***
C	0.017	1	0.017	58.98	0.0001	***
AB	2.025×10^{-5}	1	2.025×10^{-5}	0.068	0.8013	/
AC	7.225×10^{-5}	1	7.225×10^{-5}	0.24	0.6367	/
BC	2.723×10^{-4}	1	2.723×10^{-4}	0.92	0.3698	/
A ²	3.670×10^{-3}	1	3.670×10^{-3}	12.38	0.0097	***
B ²	3.060×10^{-4}	1	3.060×10^{-4}	1.03	0.3435	/
C ²	4.424×10^{-6}	1	4.424×10^{-6}	0.015	0.9062	/
Residual	2.075×10^{-3}	7	2.965×10^{-4}	/	/	/
Lack of fit terms	1.629×10^{-3}	3	5.428×10^{-4}	4.86	0.0804	/
Error	4.468×10^{-4}	4	1.117×10^{-4}	/	/	/
Total	0.35	16	/	/	/	/

Note: “****” refers to this value having an extreme influence on threshing loss rate or grain breakage rate and “/” refers to this value having no influence.

According to Tables 9 and 10, all statistical analyses were performed using SPSS Statistics Version 20 for Windows (IBM Corporation, Armonk, NY, USA). The normal distribution was verified by the Shapiro–Wilk test and homogeneity of variance was verified by Levine’s test. The results showed that the data satisfied normal distribution and variances. The *p*-values of the threshing loss rate regression model and grain breakage rate regression model are smaller than 0.0001, less than the classical confidence level of 0.05, which indicates that the assumed linear relationship of the model is reasonable and adequate, there is a significant difference with statistical significance. To verify the validity of significance, Post Hoc tests of the main effects were carried out by SPSS, as shown in Table 11. The method of least significant difference (LSD) was used for the back testing. As for threshing loss rate: (1) The differences between level −1 (52.35 rad/s) and level 1 (94.23 rad/s), as well as level 0 (73.30 rad/s) and level 1 (94.23 rad/s) of factor A-threshing cylinder speed had extreme significance. (2) There was no significant difference among the levels of factor B-concave plate speed. (3) There was no significant difference among

the levels of factor C-guide plate angle. As for grain breakage rate: (4) The differences between level -1 (52.35 rad/s) and level 0 (73.30 rad/s), as well as level 0 (73.31 rad/s) and +1 (94.23 rad/s) of factor A-threshing cylinder speed had extreme significance. (5) The differences between level 0 (10.47 rad/s) and level 1 (15.71 rad/s), as well as level -1 (5.24 rad/s) and level 1 (15.71 rad/s) of factor B-concave plate speed were significant. (6) The differences between the levels of factor C-guide plate angle were not significant.

Table 10. ANOVA of the grain breakage rate.

Source	Standard Deviation	Freedom	Sum of Squares	F Value	p Value	Significant Degree
Regression model	3.454×10^{-3}	9	3.838×10^{-4}	13.74	0.0006	***
A	8.611×10^{-4}	1	8.611×10^{-4}	30.83	0.0003	***
B	1.152×10^{-3}	1	1.152×10^{-3}	41.24	0.0002	***
C	4.961×10^{-4}	1	4.961×10^{-4}	17.76	0.0054	***
AB	1.822×10^{-4}	1	1.822×10^{-4}	6.52	0.0262	**
AC	9.000×10^{-6}	1	9.000×10^{-6}	0.32	0.1627	/
BC	6.250×10^{-6}	1	6.250×10^{-6}	0.22	0.6191	/
A ²	7.281×10^{-4}	1	7.281×10^{-4}	26.06	0.0014	***
B ²	8.253×10^{-6}	1	8.253×10^{-6}	0.30	0.3169	/
C ²	5.158×10^{-7}	1	5.158×10^{-7}	0.018	0.5490	/
Residual	1.956×10^{-4}	7	2.794×10^{-5}	/	/	/
Lack of fit terms	1.168×10^{-4}	3	3.892×10^{-5}	1.98	/	/
Error	7.880×10^{-5}	4	1.970×10^{-5}	/	0.3642	/
Total	3.650×10^{-3}	16	/	/	/	/

Note: “****” refers to this value having an extreme influence on threshing loss rate or grain breakage rate, “***” refers to this value having influence, and “/” refers to this value having no influence.

After linear regression of the model, the goodness of fit of the regression model coefficients is evaluated, and the value range is [0, 1]. The closer the coefficient is to 1, the better the fitting degree of the model is, and the more reliable the test results are. In Table 9, the determination coefficient of the model of the threshing loss rate R^2 is 0.9864, while in Table 10, the determination coefficient of the model of the grain breakage rate R^2 is 0.9696, which reflects that the regression models are good, the test results are reliable and correct.

Lack of fit is the expression of a poor model, and the lack of fit test is to check whether the measurement model lacks fit. If the p -value of the lack of fit is greater than 0.05, this indicates that the lack of fit is not significant. Otherwise, it suggests that the model is poor and cannot be used to analyze the data. The lack of fit terms of the two regression models is 0.0804 and 0.3642, which are greater than 0.05, indicate that no other factors in the model impacted the value of the threshing loss rate and grain breakage rate. The standard residual error of the regression is analyzed by Design Expert software, which satisfies the hypothesis of normality and normal distribution, and the variance is equal, indicating that the model is stable and effective, as shown in Figure 11a,b.

Further analysis shows that the main factors A (threshing cylinder speed), B (concave plate speed), C (guide plate angle), and Secondary item A^2 in the regression model have extremely significant effects on the threshing loss rate, while the main factors A (threshing cylinder speed), B (concave plate speed), C (guide plate angle), interaction item AB and AC, Secondary item A^2 , B^2 , and C^2 in the regression model have extremely significant effects on the grain breakage rate. Under the premise of ensuring that the fitted regression model is optimized and fitted, the model is obtained after eliminating the non-influencing factors, as shown in Equations (7) and (8).

$$R_1 = 4.10 - 0.2A - 0.022B + 0.047C - 0.03A^2 \tag{7}$$

$$R_2 = 0.86 + 0.0075A + 0.011B - 0.011C - 0.063AB + 0.047AC + 0.012A^2 + 0.01B^2 - 0.044C^2 \tag{8}$$

where R_1 is threshing loss rate, %; R_2 is grain breakage rate, %.

The response surface of the interaction factor to the threshing loss rate is shown in Figure 12.

Table 11. Results of Post Hoc tests of ANOVA.

Indexes	Projects	Levels	p Values	
Threshing loss rate (%)	A—threshing cylinder speed (rad/s)	-1	0	0.001
			1	0.000
		0	-1	0.001
			1	0.000
		1	-1	0.000
			0	0.000
	B—concave plate speed (rad/s)	-1	0	0.650
			1	0.190
		0	-1	0.650
			1	0.250
		1	-1	0.190
			0	0.250
C—guide plate angle (°)	-1	0	0.222	
		1	0.051	
	0	-1	0.222	
		1	0.162	
	1	-1	0.051	
		0	0.162	
Grain breakage rate (%)	A—threshing cylinder speed (rad/s)	-1	0	0.003
			1	0.093
		0	-1	0.003
			1	0.001
		1	-1	0.093
			0	0.001
	B—concave plate speed (rad/s)	-1	0	0.897
			1	0.026
		0	-1	0.897
			1	0.013
		1	-1	0.026
			0	0.013
C—guide plate angle (°)	-1	0	0.109	
		1	0.059	
	0	-1	0.109	
		1	0.473	
	1	-1	0.059	
		0	0.473	

As shown in Figure 12a,b, as the threshing cylinder speed and concave plate speed increase, the threshing loss rate decreases, and the grain breakage rate decreases slightly and then increases. This is because the contact between oilseed rape and threshing elements is sufficient when speed is low, and the grains are almost entirely removed from stalks. However, it also leads to a greater force of grain–grain impact, resulting in the grain being broken due to friction and extrusion. When the speed is high, the threshing elements and concave plate have a greater force on grains, resulting in another form of grain breakage due to impact and rubbing. Although the biological characteristics of different crops are different, there are similarities in this change rule. For example, in research on a millet threshing device by Li et al. [38], they also reached a similar conclusion. They agreed that the increased drum speed increases the speed of the millet in the threshing device, the force becomes larger, and it is easier to produce breakage and loss.

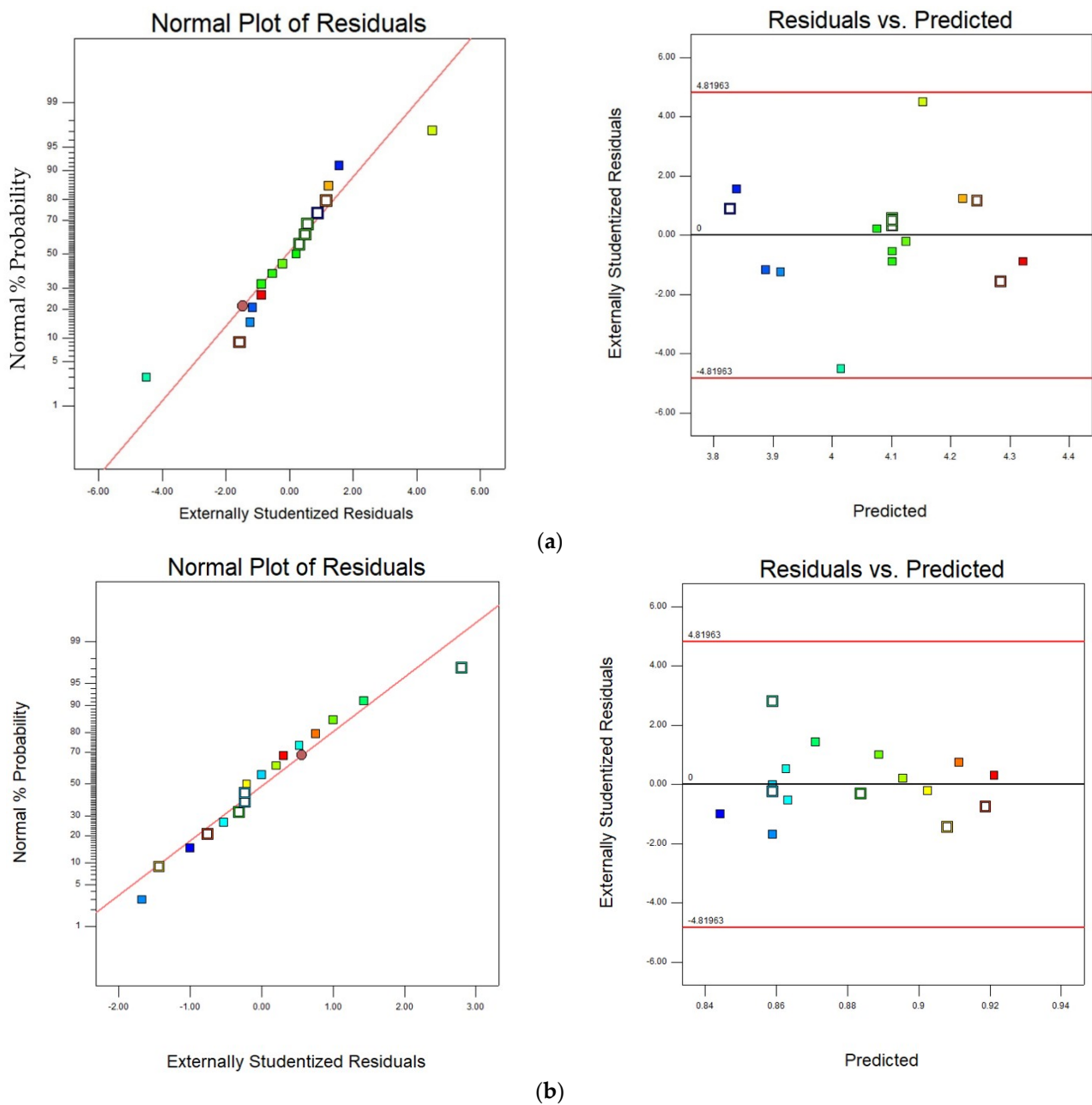


Figure 11. Standard residual error of the regression models. (a) Standard residual verification of the threshing loss rate; (b) Standard residual verification of the grain breakage rate.

Similarly, in Figure 12c,d, with the increase of guide plate angle, the threshing loss decreases, while grain breakage rate is first reduced and then increases. According to the structure of the guide plate, the similar the angle, the longer the time of the oilseed rape threshing process, the more complete the threshing effect, and the lower the threshing loss rate. Meanwhile, the dispersal ability of the threshing device to oilseed rape is better. However, with the increase of the threshing cylinder speed, the threshing cylinder gains a high speed to complete the threshing process quickly and produces a greater force on the grains, resulting in an apparent grain breakage phenomenon. Price et al. [2] pointed out that the total loss of oilseed rape harvester for them is 4.9%, and the threshing loss rate of the test results is about 1%, which greatly reduces the pod loss in the threshing process.

As shown in Figure 12e,f, the interaction of guide plate angle and concave plate speed has no significant effect on the threshing loss rate and grain breakage rate. With the increase of concave plate speed and guide plate angle, the threshing loss rate and grain breakage

rate show an overall trend of gradual increase, indicating that the greater concave speed and guide plate angle are not conducive to the oilseed rape threshing operation. In a research study by Fan et al. [39], the function of the guide plate is to prevent grains from staying and accumulating in the threshing device to avoid blockage. Generally, the guide plate angle for corn ears is about 35° , which is determined by the fact that corn ears have many bracts. A larger guide plate angle will shorten the threshing process. However, for oilseed rape threshing, the grain size is smaller than that of corn ears, so, understandably, there is a gap between this result and the literature.

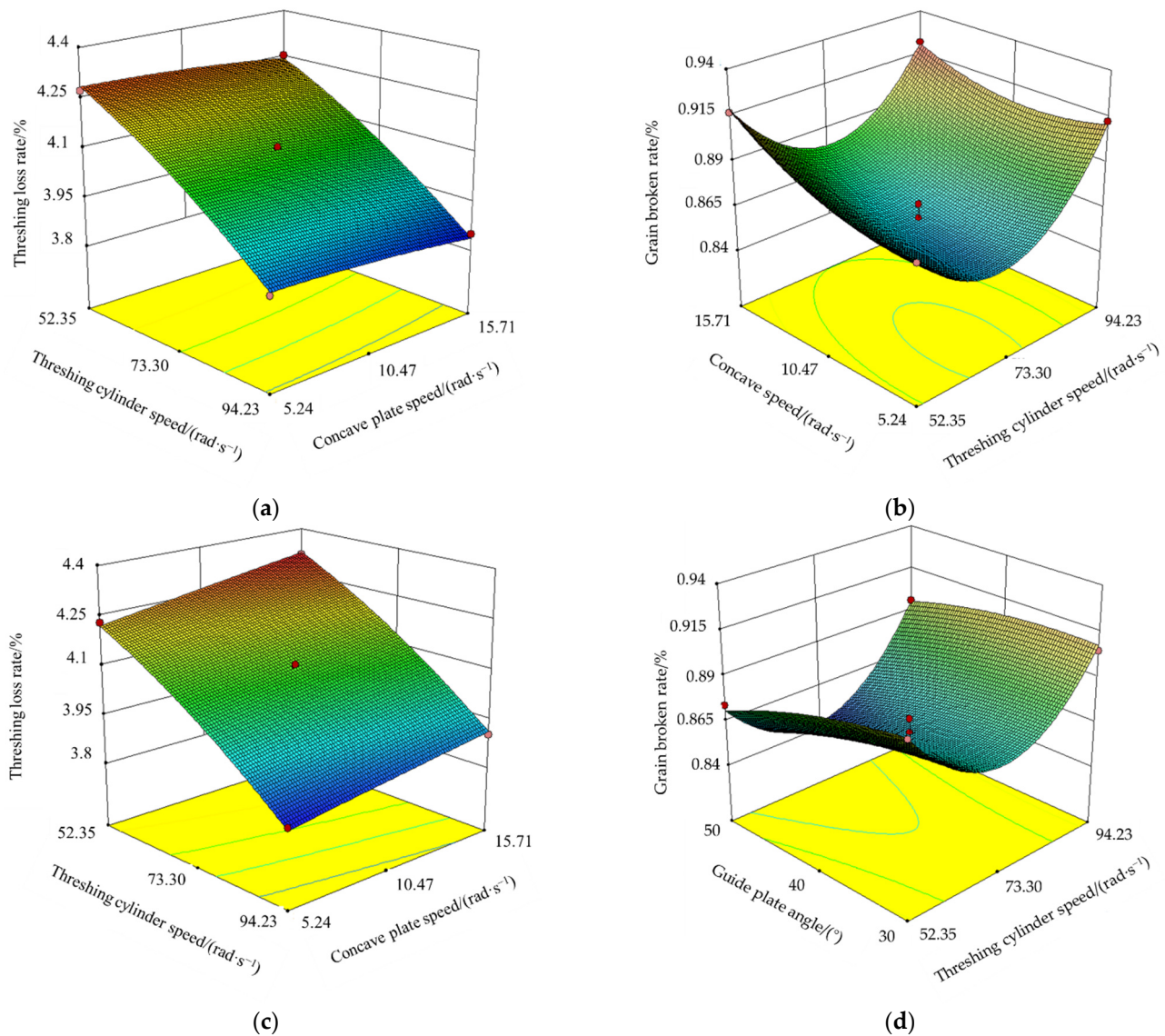


Figure 12. Cont.

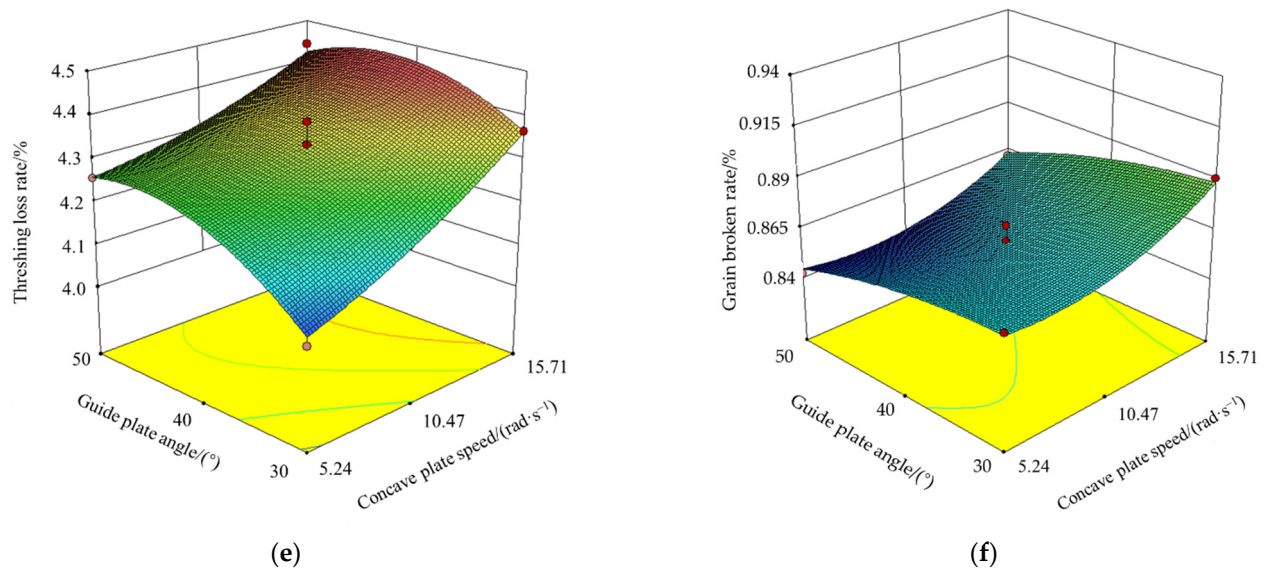


Figure 12. Influence of threshing device working parameters on threshing loss. (a) Influence of threshing cylinder speed and concave plate on threshing loss rate; (b) Influence of threshing cylinder speed and concave plate speed on grain breakage rate; (c) Influence of threshing cylinder speed and guide plate angle on threshing loss rate; (d) Influence of threshing cylinder speed and guide plate angle on grain breakage rate; (e) Influence of concave plate speed and guide plate angle on threshing loss rate; (f) Influence of concave plate speed and guide plate angle on grain breakage rate.

3.3. Optimal Parameter Design and Verification

The optimal parameter combination is determined by the action rules of each parameter on the threshing loss rate and grain breakage rate. Design Expert version 10 was used for parameter optimization design, and the optimization rule was shown in Equations (9)–(14).

$$4.068 \leq R_1 \leq 4.443 \quad (9)$$

$$0.809 \leq R_2 \leq 0.868 \quad (10)$$

$$\min R_1, R_2 \quad (11)$$

$$\text{s.t } 52.35 \leq A \leq 94.23 \quad (12)$$

$$\text{s.t } 5.24 \leq B \leq 15.71 \quad (13)$$

$$\text{s.t } 30 \leq C \leq 50 \quad (14)$$

The optimization results show that the threshing loss rate is 4.02% and grain breakage rate is 0.87% when the threshing cylinder speed is 81.89 rad/s, concave plate speed is 9.34 rad/s, and guide plate angle is 40°.

To verify the optimization results, taking the optimized parameters as the operating parameters of oilseed rape combine harvester, and the threshing loss rate and grain breaking rate as the evaluation indexes, a comparative experiment of oilseed rape harvest with 180° concave and 360° concave was conducted. The field test of each threshing concave plate was repeated five times. The test results are shown in Table 12.

As shown in Table 12, when the oilseed rape combine harvester is loaded with a threshing concave plate with a 180° wrap angle and a 360° wrap angle, the average threshing loss rate is 6.42% and 4.25%, respectively, a reduction of 2.17%, while the grain breakage rate is 2.58% and 0.93%, respectively, a decrease of 1.65%. The harvesting efficiency is 0.91 km/h and 1.03 km/h, an increase of 0.31 km/h. It improves the harvesting efficiency of the oilseed rape harvester. The standard variance results show that the 360° wrap angle threshing concave plate has a more stable working performance and is more suitable for oilseed rape threshing operations. In a research study by Teng et al. [34], they divided the

threshing concave plate with a 360° wrap angle into three parts and observed the distribution and operation effect of the threshing mixture through a bench test. Unfortunately, they did not point out how much the separation performance of the threshing concave plate was improved, and their threshing concave plate was also non-rotatable. Bruce et al. [40] found that when the threshing cylinder speed reached 80 rad/s, the grain breakage rate of oilseed pods exceeded 5%, while the threshing cylinder speed reached 100 rad/s, and the grain breakage rate exceeded 14%. The threshing concave plate designed in this study obviously reduced this value. This research not only realized the rotation of the threshing concave but also carried out verification analysis by field experiment, which made the results more intuitive.

Table 12. Field test results.

Number	Concave Plate with 180° Wrap Angle			Concave Plate with 360° Wrap Angle		
	Threshing Loss Rate (%)	Grain Breakage Rate (%)	Harvesting Efficiency (km·h ⁻¹)	Threshing Loss Rate (%)	Grain Breakage Rate (%)	Harvesting Efficiency (km·h ⁻¹)
1	6.76	2.68	0.81	4.16	0.89	1.01
2	6.54	2.75	1.0	4.22	0.91	1.15
3	6.16	2.49	0.69	4.31	1.04	1.27
4	6.42	2.57	0.83	4.38	0.86	1.24
5	6.21	2.42	0.97	4.19	0.95	1.19
Average	6.42	2.58	0.86	4.25	0.93	1.17
Standard deviation	0.22	0.12	0.10	0.08	0.06	0.10

4. Conclusions

(1) Aiming at the problems of high grain breakage rate, high threshing loss rate, and low threshing efficiency in the harvesting process of oilseed rape, a rotary threshing concave with a wrap angle of 360° was proposed for the first time. At the same time, a discrete element model of oilseed rape plants was established by DEM for the first time, and a simulation analysis of the oilseed rape threshing process was carried out. The increased contact area between oilseed rape plants and the concave plate is beneficial for improving the threshing and separation efficiency of oilseed rapeseed.

(2) The rotary threshing concave plate is beneficial in reducing the movement speed of oilseed rape grains in the device, thus reducing the threshing loss. The simulation results showed that the velocity of grains was the smallest when threshing concave angle was 40°. The established simulation model of the oilseed rape plant can be used to simulate the threshing process and to explore the interaction laws of the “plant-machine” system.

(3) The orthogonal test of oilseed rape combine harvesters shows that the threshing loss rate and grain breakage rate is 4.02% and 0.87%, respectively when the threshing cylinder speed is 81.89 rad/s, the concave plate speed is 9.34 rad/s, and the guide plate angle is 40°. The field verification test indicates that the threshing loss rate and grain breakage rate is 4.25% and 0.93% at the optimized parameters, which is 2.17% and 1.65% higher than the operating performance of the concave plate with 180° wrap angle.

(4) In future oilseed rape harvester applications, the method of automatic harvest control system based on the results of this study will be explored. It is necessary to combine the control strategy to develop the oilseed rape harvest quality inspection equipment and break through the oilseed rape harvest adaptive control technology. In addition, in the subsequent research, as many oilseed rape samples as possible will be collected. The new materials and forms of threshing concave plate or threshing elements will be explored to improve the versatility of the threshing device to meet the requirements of different harvesting conditions.

Author Contributions: Conceptualization, J.W. and Z.H.; methodology, J.W. and Z.H.; software, Q.T.; validation, Q.T.; formal analysis, Z.H.; investigation, J.W. and S.M.; resources, Q.T. and S.M.; data

curation, J.W.; writing—original draft preparation, J.W.; writing—review and editing, J.W. and L.J.; visualization, L.J.; supervision, Q.T. and Z.H.; project administration, J.W.; funding acquisition, Z.H. All authors have read and agreed to the published version of the manuscript.

Funding: This research was funded by the National Key Research and Development Program of China, 2021YFD200050201, and Basic scientific research business expenses (Chinese Academy of Agricultural Sciences), S202204.

Institutional Review Board Statement: This paper is not applicable to studies involving humans or animals.

Informed Consent Statement: Not applicable.

Data Availability Statement: Not applicable.

Conflicts of Interest: The authors declare no conflict of interest.

References

1. National Bureau of Statistics of China. *China Statistical Yearbook in 2021*; China Statistics Press: Beijing, China, 2021.
2. Price, J.S.; Hobson, R.N.; Neale, M.A.; Bruce, D.M. Seed losses in commercial harvesting of oilseed rape. *J. Agric. Eng. Res.* **1996**, *65*, 183–191. [\[CrossRef\]](#)
3. Qing, Y.R.; Li, Y.M.; Yang, Y.; Xu, L.Z.; Ma, Z. Whether the complete rapeseed grains can be harvested in the appropriate harvest period directly affects the quality of rape. *Biosyst. Eng.* **2021**, *206*, 19–31. [\[CrossRef\]](#)
4. Hobson, R.N.; Bruce, D.M. PM—Power and Machinery: Seed loss when cutting a standing crop of oilseed rape with two types of combine harvester header. *Biosyst. Eng.* **2002**, *81*, 281–286. [\[CrossRef\]](#)
5. Qing, Y.R.; Li, Y.M.; Xu, L.Z.; Ma, Z.; Tian, X.L.; Wang, Z. Oilseed rape (*Brassica napus* L.) pod shatter resistance and its relationship with whole plant and pod characteristics. *Ind. Crops Prod.* **2021**, *166*, 113459. [\[CrossRef\]](#)
6. Yi, S.J.; Zhang, Y.H.; Zhang, L. Performance test of plate teeth-grid intaglio of single axial flow threshing and separating device. *J. Agric. Mech. Res.* **2011**, *33*, 120–123. [\[CrossRef\]](#)
7. Su, Z.; Li, Y.M.; Dong, Y.H.; Tang, Z.; Liang, Z.W. Simulation of rice threshing performance with concentric and non-concentric threshing gaps. *Biosyst. Eng.* **2020**, *197*, 270–284. [\[CrossRef\]](#)
8. Hu, J.P.; Wang, S.S.; Zhou, H.M.; Xie, X.L.; Zhang, R.H. Mechanical characterization of the concave plate of a threshing device based on a multi-point distribution. *J. Henan Univ. Sci. Technol. (Nat. Sci.)* **2020**, *41*, 12–19. [\[CrossRef\]](#)
9. Regier, B.D.; Matousek, R.A.; Bennett, K.E. Combine Harvester Processing System Having Adjustable Concaves on A Suspension Systalk. U.S. Patent 8133100B2, 13 March 2012.
10. Bergkamp, A.; Regier, B. Constant Pressure Concave Assembly in A Combine Harvester Processing Systalk. U.S. Patent 9220200B2, 29 December 2015.
11. Morgan, C.L.; Bruce, D.M.; Child, R.; Ladbrooke, Z.L.; Arthur, A.E. Genetic variation for pod shatter resistance among lines of oilseed rape developed from synthetic *B. napus*. *Field Crops Res.* **1998**, *58*, 153–165. [\[CrossRef\]](#)
12. Cundall, P.A.; Strack, O.D.L. Modeling of micro mechanisms in granular material. *Stud. Appl. Mech.* **1983**, *7*, 137–149. [\[CrossRef\]](#)
13. Cundall, P.A. A computer model for simulating progressive large-scale movement in blocky rock systalk. In Proceedings of the International Symposium on Rock Fracture, Nancy, France, 4–6 October 1971; p. II-8.
14. Lenaerts, B.; Aertsen, T.; Tijskens, E.; Ketelaere, D.B.; Ramon, H.; Baerdemaeker, D.J.; Saeys, W. Simulation of grain–straw separation by Discrete Element Modeling with bendable straw particles. *Comput. Electron. Agric.* **2014**, *101*, 24–33. [\[CrossRef\]](#)
15. Liu, F.Y.; Zhang, J.; Li, B.; Chen, J. Calibration of parameters of wheat required in discrete element method simulation based on repose angle of particle heap. *Trans. Chin. Soc. Agric. Eng.* **2016**, *32*, 247–253.
16. Liu, Y.B.; Li, Y.M.; Zhang, T.; Huang, M.S. Effect of concentric and non-concentric threshing gaps on damage of rice straw during threshing for combine harvester. *Biosyst. Eng.* **2022**, *219*, 1–10. [\[CrossRef\]](#)
17. Li, X.Y.; Du, Y.F.; Liu, L.; Mao, E.R.; Yang, F.; Wu, J.; Wang, L. Research on the constitutive model of low-damage corn threshing based on DEM. *Comput. Electron. Agric.* **2022**, *194*, 106722. [\[CrossRef\]](#)
18. Wang, S.S.; Lu, M.Q.; Hu, J.P.; Chen, P.; Ji, J.T.; Wang, F.M. Design and experiment of Chinese cabbage seed threshing device combined with elastic short-rasp-bar tooth. *Trans. Chin. Soc. Agric. Mach.* **2021**, *52*, 86–94. [\[CrossRef\]](#)
19. Loof, B.; Jonsson, R. Results of investigations on resistance to shedding in rape. *Sver. Utsadesforen. Tidskr.* **1970**, *80*, 193–205.
20. Thompson, K.F.; Hughes, W.G. Breeding varieties. In *Oilseed Rape*; Scarisbrick, D.H., Daniels, R.W., Eds.; Collins Professional and Technical: London, UK, 1986; pp. 32–82.
21. Chen, Z.P.L.; Wassgren, C.; Veikle, E.; Ambrose, K. Determination of material and interaction properties of maize and wheat grains for DEM simulation. *Biosyst. Eng.* **2020**, *195*, 208–226. [\[CrossRef\]](#)
22. Guan, Z.H.; Mu, S.L.; Jiang, T.; Li, H.T.; Zhang, M.; Wu, C.Y.; Jin, M. Development of centrifugal disc spreader on tracked combine harvester for oilseed rape undersowing rice based on DEM. *Agriculture* **2022**, *12*, 562. [\[CrossRef\]](#)
23. Wang, Q.R.; Mao, H.P.; Li, Q.L. Modelling and simulation of the grain threshing process based on the discrete element method. *Comput. Electron. Agric.* **2020**, *178*, 105790. [\[CrossRef\]](#)

24. Ghodki, M.B.; Kumar, K.C.; Goswami, T.K. Modeling breakage and motion of black pepper seeds in cryogenic mill. *Adv. Powder Technol.* **2018**, *19*, 1055–1071. [[CrossRef](#)]
25. Wang, Y.; Zhang, Y.T.; Yang, Y.; Zhao, H.M.; Yang, C.H.; He, Y.; Wang, K.; Liu, D.; Xu, H.B. Discrete element modelling of citrus fruit stalks and its verification. *Biosyst. Eng.* **2020**, *200*, 400–414. [[CrossRef](#)]
26. Guo, Y.; Chen, Q.S.; Xia, Y.D.; Westover, T.; Eksioğlu, S.; Roni, M. Discrete element modeling of switchgrass particles under compression and rotational shear. *Biomass Bioenergy* **2020**, *141*, 105649. [[CrossRef](#)]
27. Schramm, M.; Tekeste, M.Z. Wheat straw direct shear simulation using discrete element method of fibrous bonded model. *Biosyst. Eng.* **2022**, *213*, 1–12. [[CrossRef](#)]
28. Liu, Y.C.; Zhang, F.W.; Song, X.F.; Wang, F.; Zhang, F.Y.; Li, X.Z.; Cao, X.Q. Study on mechanical properties for corn straw of double-layer bonding model based on discrete element method. *J. Northeast. Agric. Univ.* **2022**, *53*, 45–54. [[CrossRef](#)]
29. Liao, Y.T.; Liao, Q.X.; Zhou, Y.; Wang, Z.T.; Jiang, Y.J.; Liang, F. Parameters calibration of discrete element model of fodder oilseed rape crop harvest in bolting stage. *Trans. Chin. Soc. Agric. Mach.* **2020**, *51*, 73–82. [[CrossRef](#)]
30. Ma, Z.; Traore, S.N.; Zhu, Y.L.; Li, Y.M.; Xu, L.Z.; Lu, E.; Li, Y.F. DEM simulations and experiments investigating of grain tank discharge of a rice combine harvester. *Comput. Electron. Agric.* **2022**, *198*, 107060. [[CrossRef](#)]
31. Schramm, M.; Tekeste, M.Z.; Plouffe, C.; Harby, D. Estimating bond damping and bond Young’s modulus for a flexible wheat straw discrete element method model. *Biosyst. Eng.* **2019**, *186*, 349–355. [[CrossRef](#)]
32. Ma, X.D.; Guo, B.J.; Li, L.L. Simulation and experiment study on segregation mechanism of rice from straws under horizontal vibration. *Biosyst. Eng.* **2019**, *186*, 1–13. [[CrossRef](#)]
33. Miu, I.P.; Kutzbach, H.D. Modeling and simulation of grain threshing and separation in threshing units—Part I. *Comput. Electron. Agric.* **2008**, *60*, 96–104. [[CrossRef](#)]
34. Teng, Y.J.; Jin, C.Q.; Chen, Y.P.; Wang, T.E.; Yin, X.; Ni, Y.L.; Li, Q.L.; Ning, X.J. Design and experimental research on the 360° threshing and separation device of combined harvester. *J. Agric. Mech. Res.* **2021**, *43*, 135–142. [[CrossRef](#)]
35. Wang, C.L.; Liu, Y.; Zhang, Z.H.; Zhang, Z.H.; Han, L.; Li, Y.F.; Zhang, H.; Wongsuk, S.; Li, Y.Y.; Wu, X.M.; et al. Spray performance evaluation of a six-rotor unmanned aerial vehicle sprayer for pesticide application using an orchard operation mode in apple orchards. *Pest Manag. Sci.* **2022**, *78*, 2449–2466. [[CrossRef](#)]
36. Zhang, N.; Fu, J.; Chen, Z.; Chen, X.G.; Ren, L.Q. Optimization of the process parameters of an air-screen cleaning system for frozen corn based on the response surface method. *Agriculture* **2021**, *11*, 794. [[CrossRef](#)]
37. Li, X.Y.; Du, Y.F.; Guo, J.L.; Mao, E.R. Design, simulation, and test of a new threshing cylinder for high moisture content corn. *Appl. Sci.* **2020**, *10*, 4925. [[CrossRef](#)]
38. Li, X.P.; Zhang, W.T.; Wang, W.Z.; Huang, Y. Design and test of longitudinal axial flow staggered millet flexible threshing device. *Agriculture* **2022**, *12*, 1179. [[CrossRef](#)]
39. Fan, C.L.; Zhang, D.X.; Yang, L.; Cui, T.; He, X.T.; Zhao, H.H.; Dong, J.Q. Development and performance evaluation of a guide vane inclination automatic control system for corn threshing unit based on feedrate monitoring. *Comput. Electron. Agric.* **2022**, *194*, 106745. [[CrossRef](#)]
40. Bruce, D.M.; Hobson, R.N.; Morgan, C.L.; Child, R.D. PM—Power and Machinery: Threshability of shatter-resistant seed pods in oilseed rape. *J. Agric. Eng. Res.* **2001**, *80*, 343–350. [[CrossRef](#)]